Mon. Not. R. astr. Soc. (1980) **191**, 399–410

NGC 1275 and the Perseus cluster: the formation of optical filaments in cooling gas in X-ray clusters

L. L. Cowie*, A. C. Fabian and P. E. J. Nulsen
Institute of Astronomy, Madingley Road, Cambridge CB3 0HA

Received 1979 September 19

Summary. We discuss the role of angular momentum in radiatively cooling gas flows within rich clusters of galaxies, and consider the growth rate of perturbations owing to thermal instability in such flows. The formation of the low-velocity optical filamentation surrounding NGC 1275 in the Perseus cluster is considered in the context of the model, and excitation mechanisms are discussed. We show that mass flow rates through the core of the cluster and the mass-to-light ratio for NGC 1275 can be derived from the optical observations and that the procedure is consistent with the interpretation of the X-ray observations. Similar systems of optical filamentation should be a general signature of clusters where radiative cooling of the intercluster gas is occurring, and may yield detailed information on the gas and galaxies within such clusters.

1 Introduction

Observations with high spatial and spectral resolution of the rich X-ray clusters have in some cases, such as the Perseus cluster, supported models in which the X-ray emitting gas is cooling and accreting on to the central regions of the cluster (Gorenstein *et al.* 1978; Helmken *et al.* 1978). In other clusters, such as Coma, these models do not appear to apply. It is possible that Coma typifies a less general case in which the central gas is being heated by the binary galaxy in the cluster. Alternatively the differences between the two may correspond to slightly different central cooling times arising from differences in morphology or evolutionary history of the clusters.

In those cases where the X-ray observations of the cluster do indicate a cooling flow, a natural corollary is that the cooled gas should be seen in the central regions of the cluster as optical filamentation. The cooling gas will collect on to the local minima in the cluster potential well, corresponding normally to the central galaxies of the cluster.

Observations of the dynamics, morphology and brightness of this filamentation is important for the information it can give on the rate of mass flow of gas in the clusters, on

* Permanent address: Princeton University Observatory, Princeton, New Jersey 08540, USA.

its effects on the evolution of the centrally positioned galaxies, and on the mass-to-light ratio of the central galaxies. In addition we may predict the appearance of the central cluster regions in soft X-rays, for comparison with observations at high spatial resolution, if the structure of the optical filamentation is known.

The basic models of cooling accretion flows in clusters were given by Cowie & Binney (1977) (subsequently CB) and Fabian & Nulsen (1977) (subsequently FN). These models assumed that the flows were spherically symmetric and homogeneous. The stability of the cooling flow to comoving perturbations was discussed by Fabian & Nulsen and subsequently considered in more detail by Mathews & Bregman (1978).

In the present paper we generalize previous discussions of the steady-flow models by allowing for the effects of angular momentum, which may be important in the central cooled regions. We also study the thermal stability of the flow in a general way by relaxing the assumption that the perturbations comove. We find that they are only unstable for a restricted range of initial parameters and consider situations in which cold filaments can form. The subsequent evolution and excitation of such filaments are discussed. An estimate of the mass-to-light ratio of NGC 1275 is obtained by comparing our results with the low-velocity filamentation system surrounding NGC 1275 in the Perseus cluster. Finally we summarize the various aspects of cooling accretion flows in clusters.

2 Time-independent flows with angular momentum

2.1 THEORY

In the present section we consider the effects of angular momentum on subsonic cooling flows. If angular momentum is conserved, the centrifugal force moves rapidly from being a relatively small term to being dominant at the stagnation radius, where a disc forms. Since it is unimportant over most of the flow, the motion is nearly radial and we include the additional terms in a simple fashion by use of a centrifugal pseudo-force.

We now model the subsonic accretion flow based on this modification of the system of equations given by CB. In this section only, the notation follows that paper: gas temperature t is normalized to the infall temperature $T_c = (\gamma - 1)\,\mu m_H G 4\pi\rho_{gc} r_c^2/\gamma k$, where the galaxy density $\rho_g = \rho_{gc}(1 + r^2/r_c^2)^{-3/2}$; the radius z is normalized to r_c, and the gas density z is normalized to that at r_c. Galaxies distributed according to ρ_g inject gas on a time-scale τ giving a normalized mass flow $\omega = \dot{m}(r)\,\tau/4\pi\rho_{gc} r_c^3$. The normalized angular momentum, λ, is related to the specific angular momentum of the gas l (assumed constant) by $\lambda = l/\sqrt{4\pi G\rho_{gc} r_c^4}$. The gas goes into Keplerian orbits at the stagnation radius x_s, where centrifugal and gravitational forces balance, found by solving $\lambda = x_s^{3/2} f^{1/2}(x_s)$ where

$$f(x) = \{\ln [x + (1 + x^2)^{1/2}] - x(1 + x^2)^{-1/2}\}/x^2. \tag{1}$$

This gives $\lambda = 0.4175$, 0.1304 and 0.02669 for $x_s = 1$, 0.5 and 0.2 respectively. The flow is then determined by the modified spherically symmetric time-independent equations

$$\omega = x^2 f(x) - x_\infty^2 f(x_\infty), \quad \text{(mass continuity)} \tag{2a}$$

$$\frac{1}{z}\frac{d}{dx}(zt) = -\frac{\gamma}{(\gamma - 1)}\left\{f(x) - \frac{\lambda^2}{x^3}\right\}, \quad \text{(momentum)} \tag{2b}$$

and

$$\frac{1}{x^2}\frac{d}{dx}(\omega t) + \frac{\omega}{x^2}\left\{f(x) - \frac{\lambda^2}{x^3}\right\} = -Lz^2 t^{1/2} + \frac{1}{6(1 + x^2)^{3/2}}, \quad \text{(energy)} \tag{2c}$$

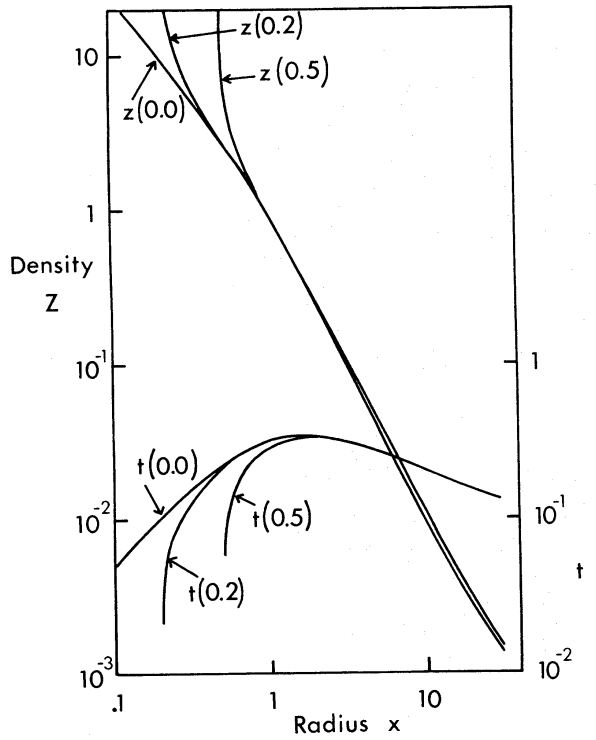

Figure 1. Normalized density z and temperature t as a function of normalized radius $x = r/r_c$. The curves represent flows which stagnate (owing to the centrifugal pseudo-force term) at $x_s = 0.0$, 0.2 and 0.5.

where the normalized cooling function (assuming bremsstrahlung cooling)

$$L = \frac{6.9 \times 10^{-28} T_c^{1/2} \tau \rho(1)^2}{4\pi r_c^2 G \mu^2 m_H^2 \rho_{gc}^2}. \tag{3}$$

These equations were solved iteratively for a given λ by searching for the appropriate value of L such that stagnation occurred at the radius x_s. The solutions are shown in Fig. 1 for both z and t.

We note that the temperature decrease inside $x = 1$ is difficult to observe because of projection effects. In Fig. 2 we show the 'projected temperature' t' found by least-squares

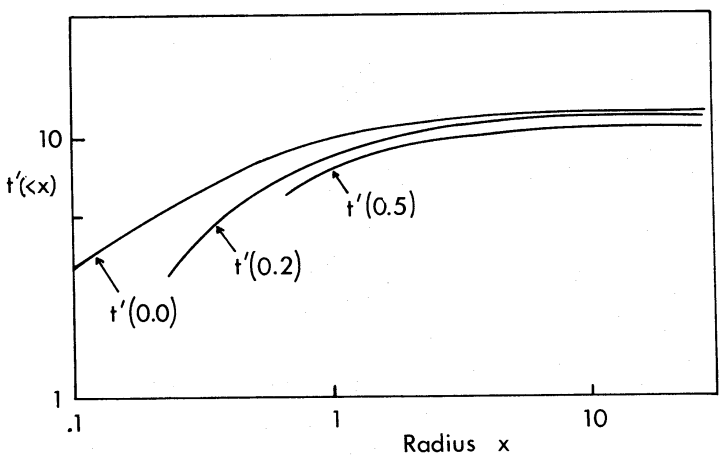

Figure 2. Projected 'temperature' t' $(<x)$ for the solutions in Fig. 1. t' is the bremsstrahlung temperature fitted to the flux emerging from within projected radii within x.

fitting of the integrated energy spectrum from radii $<x$ with a single-temperature bremsstrahlung spectrum,

$$I(E) = S(<x)/t' \exp(-E/t'),$$

where $S(<x)$ is the flux from within the projected radius x. Note that the projected temperature varies with x less steeply than t, as expected.

2.2 VISCOSITY

In the theory given above we have ignored the effects of ion viscosity which, if unimpeded, would transport angular momentum outward in the subsonic flow and enforce corotation. Quantitatively the ion mean free path (Spitzer 1962) is

$$\lambda_f = 10^4 T^2/n \quad \text{(cgs units)},$$

and for the flow time-scales, $t_{flow} \sim$ Hubble time, an unimpeded viscosity could produce corotation over dimensions $(\lambda_f v_{th} t_{flow})^{1/2} \sim 600$ kpc, where v_{th} is the thermal velocity of the gas ($\sim 10^8 \,\mathrm{cm\,s^{-1}}$) and we have set $T = 10^8$ K, $n = 10^{-3} \,\mathrm{cm^{-3}}$ for the purposes of the numerical estimate. Since this is larger than or comparable to the size of the region in which the flow time is less than a Hubble time (~ 200 kpc), viscosity is just capable of transporting the flow angular-momentum outwards.

However, there is good reason to believe that the ionic viscosity is less than this value. CB, in an analogous discussion of the stabilization of the cooling flows by electron thermal conductivity, concluded that such flows would not occur unless the conductivity was reduced by several times. A similar reduction in the viscosity is sufficient to reduce viscous transport below an interesting value. On theoretical grounds the presence of a very small tangled magnetic field would greatly reduce the effective mean free paths. The presence of such a field does not appear improbable in the converging geometry of the present systems. We note that the magnetic viscosity is unimportant unless the Alfvén velocity exceeds the velocity of sound in the gas.

2.3 QUANTITATIVE APPLICABILITY

The mass distribution within a cluster core is such that the mass within a radius r, $M(r)$, is roughly proportional to r^3 (Rood *et al.* 1972). Matter orbiting at $r < r_c$, the core radius, thus corotates with other matter $<r_c$; the orbital period P is independent of r and given by

$$P = 9 \times 10^8 n_{0.2}^{-1/2} \,\mathrm{yr}, \quad r < r_c,$$

where the number density $n = 0.2 n_{0.2} \,\mathrm{cm^{-3}}$. $n_{0.2}$ is typically ~ 1 for rich clusters. The specific angular momentum of matter orbiting at $r = 50$ kpc is then

$$l = 1.7 \times 10^4 n_{0.2}^{1/2} \,\mathrm{km\,s^{-1}\,kpc}.$$

In order to stagnate at 50 kpc, matter which is accreted from a core radius $r_c \sim 240$ kpc and conserves angular momentum must have had a transverse velocity of about $70 \,\mathrm{km\,s^{-1}}$ at r_c. This is of similar magnitude to the expected net velocity of galaxies in the core

$$v_c \simeq \sigma/\sqrt{N_g},$$

which is about 50–$100 \,\mathrm{km\,s^{-1}}$ for a velocity dispersion, $\sigma \sim 10^3 \,\mathrm{km\,s^{-1}}$, and a number of galaxies, $N_g \sim 100$. (The typical mass flow of gas to the central regions of a cluster over a

Hubble time is about 10^{12}–$10^{13} M_\odot$, so that a minimum of about 100 galaxies must have contributed to the accreted mass, while the number of luminous galaxies (~ few hundred) in the cluster sets an upper bound to the number which have contributed.) Gas stripped from the galaxies in the core of such a cluster is thus likely to stagnate and orbit at radii of about 50 kpc. Any net rotation that the cluster may have due to some other process (perhaps primordial) strengthens this conclusion.

3 Thermal instability in the cooling surface

FN pointed out that the steady-flow solutions are thermally unstable, while Mathews & Bregman (1978) analysed the growth of perturbations which remained comoving with the surrounding flow. Since relative motions of perturbations with respect to their surroundings may stabilize the thermal instability we shall generalize the perturbation analysis to include the dynamics of the perturbed 'blobs'.

The equation of motion describing the trajectory of a blob may be written

$$\rho_b \frac{d^2 r}{dt^2} = -\Delta\rho \left(\frac{GM}{r^2} - \frac{l^2}{r^3}\right) - \text{sign}\,(v_{rel}) \frac{\rho_b v_{rel}^2 \sigma_b}{V_b}, \tag{4}$$

where ρ_b is the blob density, $\Delta\rho$ the difference between the blob density and the external density, v_{rel} the blob's velocity relative to its surroundings, σ_b its effective drag cross-section and V_b its volume. The first term on the RHS of equation (4) represents the effective gravitational force while the second term is the drag on the blob. If we now define $\xi = \sigma_b r_c / V_b$, $t_{ff} = (4\pi G \rho_{gc})^{-1/2}$ and $\eta = \rho_{gc} t_{ff} / \rho(1)\, \tau$, we may rewrite the equation in dimensionless form as

$$\frac{d^2 x}{d\theta^2} = -\frac{(z - z_0)}{z}\left\{f(x) - \frac{\lambda^2}{x^3}\right\} - \xi_i \frac{z_0}{(z_i z^2)^{1/3}}\left(\frac{dx}{d\theta} - \frac{\eta\omega}{z_0 x^2}\right)^2 \text{sign}\left(\frac{dx}{d\theta} - \frac{\eta\omega}{z_0 x^2}\right) \tag{5}$$

where we have defined the dimensionless time $\theta = t/t_{ff}$. Here ξ_i measures the initial dimensionless size of the blob, z_i is the initial density in the blob, and subscript 0 now refers to quantities in the unperturbed flow.

The density evolution of the blob may be determined from the energy equation

$$\rho_b T_b \frac{dS_b}{dt} = -n_b^2 \Lambda(T_b), \tag{6}$$

where S_b is the specific entropy of the blob. In dimensionless form this becomes:

$$\frac{dz}{d\theta} = \eta L \left(\frac{z^5}{z_0 t_0}\right)^{1/2} - \frac{3}{2}\frac{z}{t_0}\frac{dx}{d\theta}\left(f(x) - \frac{\lambda^2}{x^3}\right). \tag{7}$$

The evolution of a blob is determined by the radius x_i at which it is introduced, with velocity v_i and density z_i, together with the size parameter ξ_i and η. This last quantity measures the ratio of the gravitational infall time, t_{ff}, to the flow time and has the value

$$\eta = 1.25 \times 10^{-3}\, \dot{m}_{300}^{1/2} t_8^{3/2} r_{240}^{-2}$$

for the flows discussed in Section 2. We have used the eigenvalue L to determine $\rho_{gc}/\rho(1)$; the total mass-flow rate is $300 \dot{M}_{300} M_\odot\,\text{yr}^{-1}$; t_{ff} is $10^8 t_8$ yr and $r_c = 240 r_{240}$ kpc. The smallness of η means that it is relatively easy for a blob to attain its terminal velocity, which is

(neglecting centrifugal force)

$$\dot{x}_t = [(\alpha - 1) f(x)/\xi]^{1/2},$$

where $\alpha = z(x)/z_0(x)$.

The blob then moves towards that part of the flow which is of similar entropy. The blob is thermally stable (relative to the flow) if it can reach this equilibrium position before cooling. A small perturbation must move a distance

$$\Delta x \simeq \frac{S_0 - S}{dS_0/dx} = \frac{(\alpha - 1)\,\omega t_0^{1/2}}{L z_0^2 x^2}$$

relative to the flow, giving a stability criterion

$$\frac{\Delta x}{\dot{x}_t} < \frac{x}{\dot{x}_0}, \tag{8}$$

or

$$(\alpha - 1) < \frac{x_i^{10} z_0^6 f(x_i)\, L^2}{t_0 \omega_i^4} (\eta \xi^{1/2})^{-2}.$$

This condition is shown for $x_i = 1$ in Fig. 3. A perturbation of higher density-contrast cools on a significantly shorter time-scale than the surrounding medium, requiring

$$\alpha \lesssim \frac{f^{1/2}(x)\, t_0^{1/2}}{L z_0} (\eta \xi^{1/2})^{-1}. \tag{9}$$

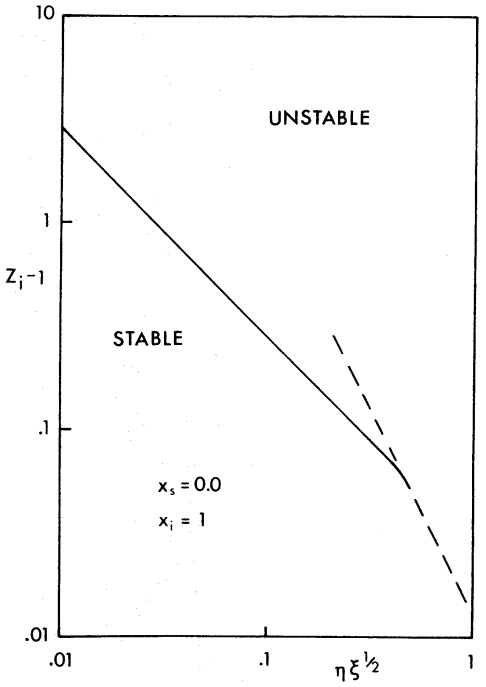

Figure 3. Region of instability for $x_i = 1$ and $x_s = 0.0$. As discussed in the text for small η this can be expressed in terms of the density contrast $\alpha - 1$ ($= z_i - 1$ here) and the parameter $\eta\xi^{1/2}$ which determines the ratio of the unperturbed flow velocity to the terminal velocity at a given x. The dashed line represents the condition (8) for small perturbations and the full line, obtained from numerical calculation, is essentially condition (9).

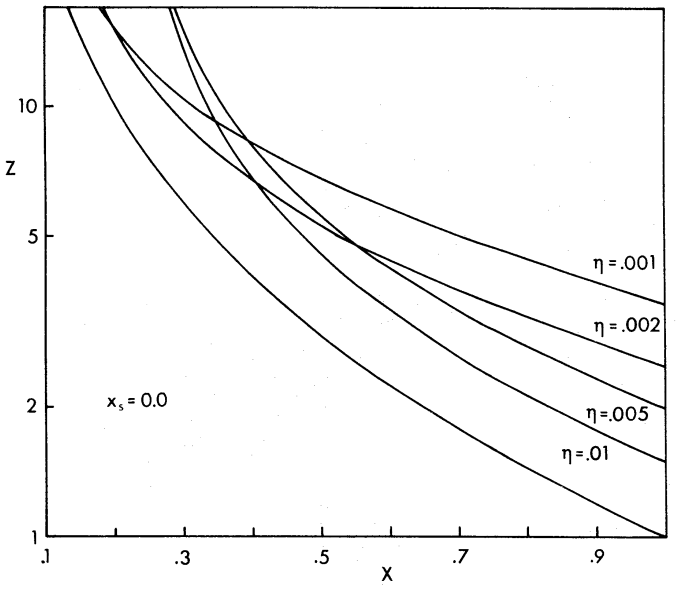

(a)

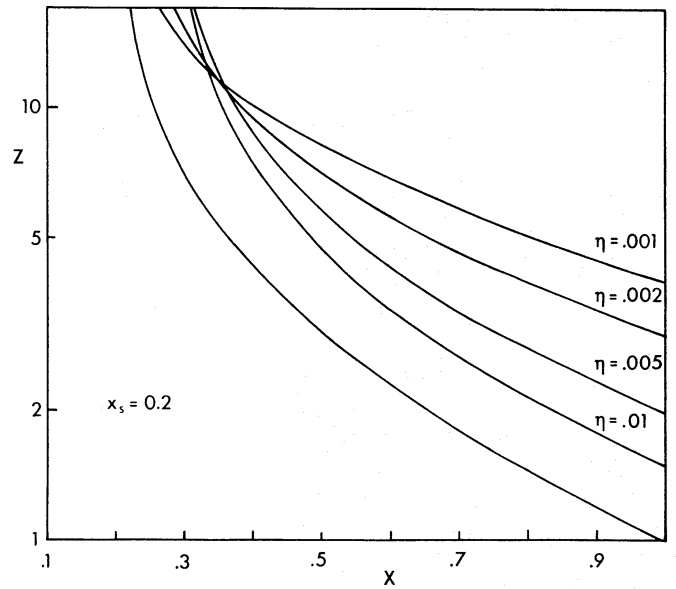

(b)

Figure 4. Growth of perturbations in radiatively cooling flows. In (a) $x_S = 0.0$ and in (b) $x_S = 0.2$. In each figure, $z(x)$ is plotted against x for marginally unstable blobs with $\xi_i = 100$ and for various η between 0.01 and 0.001. The curve at the bottom is z for the unperturbed flow.

However, now $\Delta x \sim x$ and the above condition has limited meaning. We have thus integrated the perturbation equations numerically for various η, ξ_i and z_i from $x_i = 1$, injecting the blobs at their terminal velocity. The results have been used to complete Fig. 3. We show $z(x)$ for some marginally unstable cases in Fig. 4, where $x_s = 0.0$ and 0.2.

Since the cooling time within the core is roughly equal to the flow time, both the stability conditions (8) and (9) can be expressed there approximately as $\dot{x}_0 \lesssim \dot{x}_t$. $\dot{x}_0$ increases with decreasing x, whereas $\dot{x}_t$ decreases, making stability more difficult to satisfy deeper within the core (Fig. 5). Near the stagnation radius we expect all blobs to be unstable, giving rise to a chaotic situation.

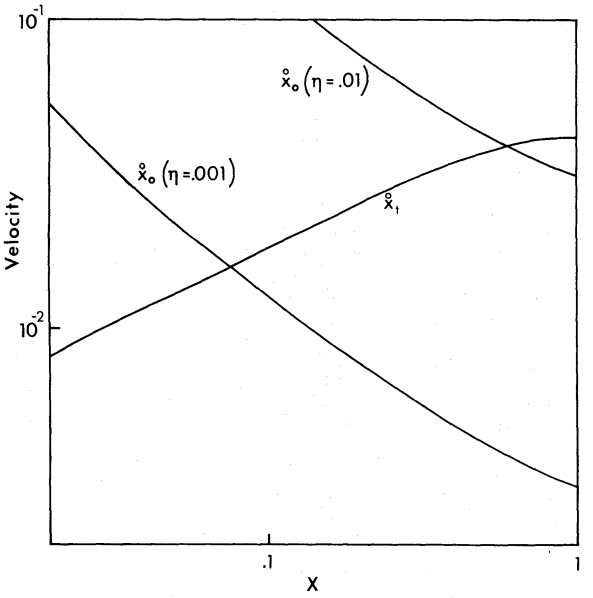

Figure 5. Stability as a function of position in the flow. $\dot{x}_t$, the terminal velocity of a blob with $\alpha = 2$, and $\xi = 100$, is plotted along with $\dot{x}_0$ the velocity in the unperturbed flow with $x_s = 0$ and $\eta = 0.01$ and 0.001. As discussed in the text, the stability criterion $\dot{x}_0 \lesssim \dot{x}_t$ becomes more difficult to satisfy deeper in the flow so that blobs injected there are less likely to be thermally stable.

We have so far assumed that the blob is spherical. The bulk forces of gravity and buoyancy act equally on all parts of the blob whereas the drag forces act only at the inner surface. This will tend to cause the blob to be torn apart, increasing the relevant value of ξ and reducing the terminal velocity $\dot{x}_t$. Large blobs are thus expected to fragment into strings of nearly comoving blobs, in appearance similar to the non-linear development of the Rayleigh–Taylor instability. The resulting fragments are each more likely to be unstable than the original blob (Fig. 3).

Several other factors tend to make the flow produce thermally unstable blobs. Our assumption that the gas originates within the galaxies suggests that it may be very clumpy, especially where gas is injected within the core. Clumpiness in the flow effectively changes the cooling function Λ. Moreover, Λ is underestimated, and the blobs more unstable, when the temperature $\lesssim 3 \times 10^7$K, below which line cooling is effective (Raymond, Cox & Smith 1976).

We conclude this section by noting that the growth of comoving blobs, as discussed by Mathews & Bregman (1978) is only relevant to a restricted range of blob parameters. The modifications discussed above to our simple dynamical model of a blob nevertheless suggest that some cooled filaments can reasonably arise at large distances from the mean stagnation radius.

4 Filament formation and excitation

We can now form a semiquantitative picture of the gas flow in the central regions of the cluster. All gas ultimately reaches Keplerian velocities and orbits the central galaxy at the stagnation radius (around 50 kpc for typical rich clusters). The gas may enter the stagnation region either as hot ($T \sim$ few 10^7K, $n \sim 10^{-2}$cm^{-3}) subsonically inflowing material, or as cooled slightly denser lumps formed by thermal instability in the cooling interface. In the former case the cooling time must be comparable to the orbital period (around 10^9yr for

a typical rich cluster). The pressure in the hot gas at the stagnation radius is determined by the steady-state solution of the accretion flow and is approximately three times the pressure at the core radius of galaxies in the cluster (which for typical clusters corresponds to $nT \sim 2 \times 10^6\,\mathrm{K\,cm^{-3}}$) and is relatively insensitive to the angular momentum parameter (*cf.* Fig. 1).

The final stages of filament cooling are isochoric rather than isobaric, the cooled gas returning to pressure equilibrium with the surrounding hot material by passage of a shock-wave through the clump (Mathews & Bregman 1978). For temperatures larger than $2 \times 10^7\,\mathrm{K}$ the cooling function is approximately thermal bremsstrahlung (Raymond *et al.* 1976), and the cooling time in a clump of density n_{cl}

$$t_{\mathrm{cool}} = 5.2 \times 10^{16} \frac{T_7^{1/2}}{n_{-2}}\ \mathrm{s}, \tag{10}$$

where n_{-2} is the clump density in units of $10^{-2}\,\mathrm{cm^{-3}}$. At lower temperatures ($10^5\,\mathrm{K} < T < 2 \times 10^7\,\mathrm{K}$) for a gas with heavy element abundances of approximately one-half the cosmic value, we can approximate the cooling function by a power-law form $\Lambda = 3 \times 10^{-19} T^{-0.6}\,\mathrm{erg\,cm^3\,s^{-1}}$ (McKee & Cowie 1977), when the cooling time becomes

$$t_{\mathrm{cool}} = 2.2 \times 10^{16} \frac{T_7^{1.6}}{n_{-2}}\ \mathrm{s}. \tag{11}$$

Setting this equal to the crossing time for sound within the cloud, the cooling becomes isochoric when

$$T = 3 \times 10^6 \{d(n_{\mathrm{ext}}T_{\mathrm{ext}})_6\}^{0.32}\,\mathrm{K}, \tag{12}$$

where d is the dimension of the clump in kpc and $(n_{\mathrm{ext}}T_{\mathrm{ext}})_6$ is the outside pressure in units of $10^6\,\mathrm{K\,cm^{-3}}$. The shock velocity with which the cloud is repressurized is approximately equal to the sound speed at the temperature at which the cloud became isochoric. Setting $\rho_{\mathrm{cl}} V_{\mathrm{sh}}^2 = 1.7 k_{\mathrm{B}} (n_{\mathrm{ext}}T_{\mathrm{ext}})$ we obtain

$$V_{\mathrm{sh}} = 210 \{d(n_{\mathrm{ext}}T_{\mathrm{ext}})_6\}^{0.16}\ \mathrm{km\ s^{-1}}, \tag{13}$$

where the preshock clump density

$$n_{\mathrm{cl}} = 0.3 \frac{(n_{\mathrm{ext}}T_{\mathrm{ext}})_6^{0.68}}{d^{0.32}}\ \mathrm{cm^{-3}}. \tag{14}$$

Using the simple formula given by Cowie & York (1978), the post-shock surface brightness in the Hα line is

$$S(\mathrm{H}\alpha) = 2.5 \times 10^{-6} d^{0.16} (n_{\mathrm{ext}}T_{\mathrm{ext}})_6^{1.16}\ \mathrm{erg\ cm^{-2}\ s^{-1}\ sr^{-1}}. \tag{15}$$

It may be seen that this is sensitive principally to the external pressure.

Two further points on the filament emission should be noted. The total energy which can be directly radiated from the isochorically cooling clumps at low temperatures ($T \sim 10^4\,\mathrm{K}$) is small, being about 10^{-4} of the X-ray luminosity or a few times $10^{40}\,\mathrm{erg\,s^{-1}}$ for a very luminous cluster (CB, FN, Kent & Sargent 1979). Secondly, only a small fraction ($\sim 10^5 M_\odot$) of the total mass of material which has passed into the clumps ($\approx 10^{13} M_\odot$) can remain as ionized gas in pressure equilibrium with the surroundings, since otherwise the cluster would be very luminous optically. The remaining material must form into stars, cool and become neutral, or be disposed of in some other way.

The velocity dispersion of the filamentation measures the Keplerian velocity and hence determines the gravitating mass within the filaments. That is

$$M_{\rm grav}(r) = r v_{\rm disp}^2 / G \sin^2 i, \tag{16}$$

where r is the radius at which the filaments form.

5 NGC 1275 and the Perseus cluster

Kent & Sargent (1979) give the surface brightness of the optical filamentation in the NGC 1275 low-velocity filamentation system, which we identify as gas accreting on to NGC 1275 from cooling gas from the Perseus cluster, as $S(\mathrm{H}\alpha) = 1.6 \times 10^{-5}\,\mathrm{erg\,cm^{-2}\,s^{-1}\,sr^{-1}}$. The spectrum is consistent with the line-emission ratios which would be expected behind a shock with a velocity of $100\,\mathrm{km\,s^{-1}}$, and the pressure in the gas may be inferred from the S II line ratios, giving $(nT) = 1.2 \times 10^7 T_4^{3/2}\,\mathrm{K\,cm^{-3}}$, where T_4 is the gas temperature in units of 10^4 K. Typical sizes in the filaments can be estimated as 1–2 kpc from the Hα photograph by Lynds (1970) (assuming $H_0 = 50\,\mathrm{km\,s^{-1}\,Mpc^{-1}}$). Kent & Sargent (1979) estimate a total Hβ luminosity of $2 \times 10^{41}\,\mathrm{erg\,s^{-1}}$.

If the filaments are excited by collisional ionization following the repressurizing shock, then we can also estimate the external pressure from equation (15), obtaining $(n_{\rm ext} T_{\rm ext}) = 5 \times 10^6\,\mathrm{K\,cm^{-3}}$, which may be compared with a pressure of $9 \times 10^6\,\mathrm{K\,cm^{-3}}$ inferred from the S II line ratio if we assume $T_4 = 0.8$ in the S II emitting region. However, the estimated shock velocity is $250\,\mathrm{km\,s^{-1}}$, a value somewhat too high to agree with the observed ionization structure. The problem would be alleviated if the filaments are clumpy with much of the emission coming from slightly denser regions. This would have combined the effect of slightly increasing the pressure estimate given above, bringing it into better agreement with that estimated from the S II ratios.

The pressure may also be inferred from the X-ray observations in combination with the present theoretical model. From the results of CB we estimate that the pressure at the core radius should be $(nT) \approx 5 \times 10^5\,\mathrm{K\,cm^{-3}}$, which would rise to approximately $2 \times 10^6\,\mathrm{K\,cm^{-3}}$ at the stagnation radius. This is slightly lower than the pressures inferred from the filaments, but this might be expected since the relative motions of clumps within the thermally unsteady cooling flow can raise the pressure somewhat above that in the steady flow.

The crossing time of the shock in the optical filament is approximately 10^7 yr, shorter than the free-fall time of 10^8 yr in the Jeans-unstable cooled filament. The surface area of filaments is given as 1000 arcsec^2 by Kent & Sargent, which for a size of 1 kpc implies a volume of $10^{67}\,\mathrm{cm^3}$ and a mass of $2 \times 10^9 M_\odot$. Combined with the characteristic time-scale, this gives a mass flow rate of $200 M_\odot$/yr, very similar to that estimated on the basis of cooling time-scale arguments and X-ray observations of the cluster (CB, FN).

Kent & Sargent (1979) have pointed out that a comparable contribution to the optical luminosity may come from photo-ionization of the filaments by radiation from the Seyfert nucleus. The observed spectra are also consistent with this interpretation. If this is the dominant excitation mechanism, the estimate of the pressure based on the net optical luminosity is reduced, but other quantities calculated above remain invariant. In this case the filaments might be somewhat overpressured with respect to the surrounding gas. Additional photo-ionization may be caused by stars forming within the collapsing clump and by soft X-ray emission from the surrounding gas.

Finally we may estimate the mass of material enclosed by the filamentation system. The total velocity spread is $700\,\mathrm{km\,s^{-1}}$ (Rubin *et al.* 1978). No clear evidence for rotation can be seen, but the velocities are of the order expected from orbital motions. Using equation (16)

we estimate a mass, interior to the filaments, of $3 \times 10^{12} M_{\odot}$, where we have set $v_{\rm disp} = 350\,{\rm km\,s^{-1}}$ and $r = 100\,{\rm kpc}$. Combined with Sandage's (1972) visual luminosity of $1.3 \times 10^{11} L_{\odot}$, this gives a mass-to-light ratio $\leqslant 20/\sin^2 i$ for NGC 1275. The mass within the optical filaments is consistent with a flow rate of $200 M_{\odot}\,{\rm yr^{-1}}$ for a Hubble time and may arise almost completely from accretion.

6 Conclusion

While the above discussion has been restricted to NGC 1275 it can be seen that observations of optical filamentation in the central regions of clusters are a powerful means of studying the mass flow rates within the cluster (and hence cluster X-ray luminosities), and for investigating the mass distribution within the central regions of the cluster core. More detailed spectroscopic measurements of the filaments will ultimately give information on the metallicities, which would be substantially more difficult to obtain in the X-rays.

The occurrence of cooling filaments in a cluster of galaxies requires first that the cooling time of the gas within the core be shorter than a Hubble time. Stagnation of the subsequent cooling flow is likely to occur at ~ 50 kpc from the centre, due to the mean angular momentum within the flow. The existence and appearance of a more extensive system of filaments depends upon the history of gas injection – the density contrast, size and angular momentum of injected gas. The optical filaments provide an indication of the regions that are expected to show X-ray enhancements. They need not correlate in detail. The gas currently in filamentation occupied a volume ~ 10^3 times larger when at X-ray temperatures. Furthermore, that gas will have separated out from the general flow at some larger radius, as discussed in Section 3.

Cooled intracluster gas may contribute significantly to, or even create, slow-moving central galaxies. The extent of such galaxies may be related to the past history of mass loss by other galaxies within the cluster core. We anticipate the discovery of other systems of filamentation, similar to that around NGC 1275, in other X-ray clusters. Such finds would contribute greatly to our understanding of the evolution of intracluster gas.

Acknowledgments

We thank J. Ostriker and L. Spitzer for discussions. LLC was supported in part by NASA grants NGL-31-001-007 and NAS8-33345. ACF thanks the Radcliffe Trust for support. PEJN acknowledges receipt of an Isaac Newton Studentship.

References

Cowie, L. L. & Binney, J., 1977. *Astrophys. J.*, **215**, 723.
Cowie, L. L. & York, D. G., 1978. *Astrophys. J.*, **220**, 129.
Fabian, A. C., Zarnecki, J. C., Culhane, J. L., Hawkins, F. J., Peacock, A., Pounds, K. A. & Parkinson, J. E., 1971. *Astrophys. J.*, **189**, L59.
Fabian, A. C. & Nulsen, P. E. J., 1977. *Mon. Not. R. astr. Soc.*, **180**, 479.
Gorenstein, P., Fabricant, D., Topka, K., Harnden, F. R., Jr & Tucker, W. H., 1978. *Astrophys. J.*, **225**, 718.
Helmken, H., Delvaille, J. P., Epstein, S., Geller, M. J. & Schnopper, H. W., 1978. *Astrophys. J.*, **221**, L43.
Kent, S. M. & Sargent, W. L. W., 1979. *Astrophys. J.*, **230**, 667.
Lynds, R., 1970. *Astrophys. J.*, **159**, L151.
McKee, C. F. & Cowie, L. L., 1977. *Astrophys. J.*, **215**, 213.
Mathews, W. G. & Bregman, J. N., 1978. *Astrophys. J.*, **224**, 308.
Raymond, J. C., Cox, D. P. & Smith, B. W., 1976. *Astrophys. J.*, **204**, 290.

Rood, H. W., Page, T. L., Kintner, E. C. & King, I. R., 1972. *Astrophys. J.*, **175**, 627.
Rubin, V. C., Ford, W. K., Peterson, C. J. & Lynds, C. R., 1978. *Astrophys. J. Suppl.*, **37**, 235.
Sandage, A., 1972. *Astrophys. J.*, **178**, 1.
Spitzer, L., Jr, 1962. *Physics of Fully Ionized Gases*, Interscience, New York.